

## Proton conductivity of perfluorosulfonate ionomers at high temperature and high relative humidity

Bruno R. Matos, Cleverton A. Goulart, Elisabete I. Santiago, R. Muccillo, and Fabio C. Fonseca

Citation: [Applied Physics Letters](#) **104**, 091904 (2014); doi: 10.1063/1.4867351

View online: <http://dx.doi.org/10.1063/1.4867351>

View Table of Contents: <http://scitation.aip.org/content/aip/journal/apl/104/9?ver=pdfcov>

Published by the [AIP Publishing](#)

---

The cover of the 'Multiphysics Simulation' e-magazine features a photograph of a complex electronic circuit board. The text on the cover includes 'MULTIPHYSICS SIMULATION' at the top, 'SPECTRUM' in a small box, and 'SIMULATION ADVANCES DESIGN AT ABB' at the bottom right.

**FREE Multiphysics Simulation e-Magazine**

**DOWNLOAD TODAY >>**

The COMSOL logo consists of a small square icon followed by the word 'COMSOL' in a bold, sans-serif font.

## Proton conductivity of perfluorosulfonate ionomers at high temperature and high relative humidity

Bruno R. Matos, Cleverson A. Goulart, Elisabete I. Santiago, R. Muccillo, and Fabio C. Fonseca

*Instituto de Pesquisas Energéticas e Nucleares, IPEN-CNEN, Avenida Prof. Lineu Prestes, 2242, São Paulo (SP) 05508000, Brazil*

(Received 18 January 2014; accepted 20 February 2014; published online 4 March 2014)

The proton transport properties of Nafion membranes were studied in a wide range of temperature by using an air-tight sample holder able to maintain the sample hydrated at high relative humidity. The proton conductivity of hydrated Nafion membranes continuously increased in the temperature range of 40–180 °C with relative humidity kept at  $RH = 100\%$ . In the temperature range of 40–90 °C, the proton conductivity followed the Arrhenius-like thermal dependence. The calculated apparent activation energy  $E_a$  values are in good agreement with proton transport via the structural diffusion in absorbed water. However, at higher measuring temperatures an upturn of the electrical conductivity was observed to be dependent on the thermal history of the sample.

© 2014 AIP Publishing LLC. [<http://dx.doi.org/10.1063/1.4867351>]

The perfluorosulfonate ionomer membranes such as Nafion possess a high water sorption capacity and one of the highest proton conductivity at low temperature among solid proton conductors.<sup>1</sup> Due to the importance of such electrolytes in polymer electrolyte membrane fuel cells (PEMFCs), chlor-alkali production, and in electroactive polymer actuators, strong research efforts have been dedicated to investigate the effect of water sorption on the microstructure and electrical properties of Nafion membranes using numerous techniques.<sup>1,2</sup> The proton conductivity and diffusion coefficient in water-swollen Nafion membranes are  $\sigma \sim 10^{-1} \text{ S cm}^{-1}$  and  $D \sim 10^{-5} \text{ cm}^2 \text{ s}^{-1}$ , respectively.<sup>3</sup> Such high values have been attributed to (i) the high dissociation constant of sulfonate groups in aqueous solution; (ii) the low percolation threshold of the hydrophilic phase; and (iii) the nanophase separated morphology of Nafion.<sup>1,4–6</sup> Although much information on the electrical properties of perfluorosulfonate ionomers has been collected over the years, the proton conduction properties at high temperature ( $T > 100^\circ\text{C}$ ) and at high relative humidity ( $RH = 100\%$ ) have been seldom reported.<sup>3</sup> Proton conductivity measurements at  $T > 100^\circ\text{C}$  have been performed mostly under reduced  $RH$  (constant water partial pressure).<sup>3</sup> Such studies revealed that at  $T > 100^\circ\text{C}$  the proton conductivity decreases due to desorption of water from the ionomer matrix, which blocks the conduction pathways available for the ion migration via Grotthuss mechanism.<sup>3</sup> On the other hand, Nafion water sorption was reported to increase with increasing temperature at high (and constant) relative humidity.<sup>7</sup> PEMFCs operate continuously at high  $T$  and  $RH$  and the characterization of Nafion proton conductivity in such conditions is crucial for the development of new ionomer membranes aiming at increasing PEMFC efficiency.<sup>3,8,9</sup>

In the present study, a home-made air-tight sample holder was built allowing the measurements of proton conductivity at high  $T$  and  $RH$ . Impedance spectroscopy (IS) data of Nafion membranes were carefully collected in a wide range of temperature and frequency at high relative humidity ( $RH = 100\%$ ).

Commercial Nafion membranes with different equivalent weight (EW), Nafion 105 ( $EW = 1000 \text{ g Eq}^{-1}$ ) and 115 ( $EW = 1100 \text{ g Eq}^{-1}$ ), were obtained from Dupont. The membranes were post-treated by standard cleaning and activation protocols.<sup>8</sup> Samples (in the protonic form) were characterized in the hydrated form without previous thermal treatment to avoid morphological changes.

A Solartron 1260 frequency response analyzer was used for IS measurements in 4 mHz to 3 MHz frequency ( $f$ ) range with 100 mV *ac* amplitude. Further details of IS measurement are described elsewhere.<sup>10</sup> The total resistance of the samples was obtained from the intercept of the impedance semicircle at high frequencies ( $f \sim 10^6 \text{ Hz}$ ) with the real axis of the complex plane.<sup>6</sup> The IS data of Nafion membranes were collected in a specially designed air-tight sample holder.<sup>10,11</sup> Nafion samples ( $1.5 \times 1.5 \text{ cm}^2$ ) were sandwiched between stainless steel spring-load contact terminals, which are insulated from the chamber walls. Circular pieces of carbon cloth (1 cm diameter) with carbon ink (Teflon + Vulcan XC72) painted manually in both faces were placed between stainless steel contact terminals and the sample to facilitate water equilibration and improve the electrical contact with the membrane. The sample was stabilized with water vapor for 24 h at 30 °C ( $RH = 100\%$ ) prior to IS measurements. Fig. 1 shows the detailed scheme of the designed sample holder for controlling the environmental conditions for the IS measurements.

The sample holder consists of two compartments: the lower one is the water reservoir and the upper one the sample chamber. These compartments are physically separated and thermally insulated by a teflon disc. This setup is tightly sealed with Viton gaskets and screws to prevent vapor leakage. To control the  $RH$  of the sample, the temperature of both the water reservoir and sample chamber are independently adjusted by band-heaters connected to temperature controllers. This setup allows controlling the dew point for IS measurements in a broad range of  $T$  and  $RH$ . The  $RH = 100\%$  is nominally achieved when the lower and upper compartments have the same  $T$ . In this condition, the rates of

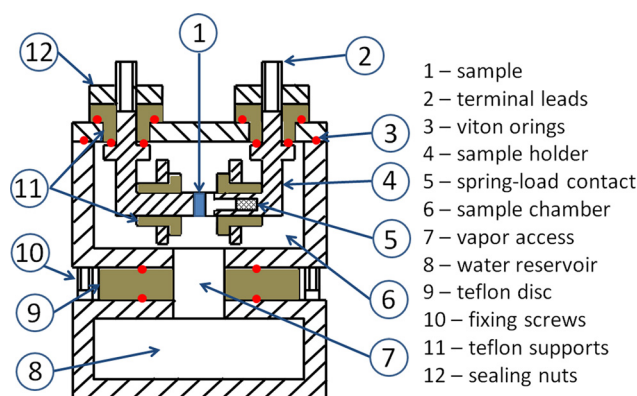


FIG. 1. Schematics of the designed sample holder for controlling the environmental conditions for impedance spectroscopy measurements at high  $RH$  and  $T$ .

evaporation and condensation are equivalent. However, thermal fluctuations of the band heaters can result in accumulation of condensed water, which can result in misleading conductivity data. Thus, to avoid water accumulation in the sample-holder, the sample is positioned vertically. No abrupt variations of proton conductivity were observed and no liquid water was found on the sample chamber after IS measurements, thus indicating the absence of condensed water in the setup. To compare the measurements performed with the designed sample holder, IS measurements were also performed as a function of temperature at  $RH = 100\%$  in the in-plane configuration (two-probe) with a commercial sample holder (FuelCon<sup>®</sup> TrueXessory-PCM).

Prior the analysis of the temperature dependence of the proton conductivity, both the resistance of the short-circuited sample holder (containing two carbon electrodes) and the resistance of the electrode-membrane interfaces in the through-plane configuration were determined. Previous studies of the proton transport of Nafion membranes revealed that if the parasitic (extrinsic) resistances are neglected it can result in misleading values of both conductivity and activation energies.<sup>12</sup> Such parasitic resistances can be eliminated from the IS data by separating the resistance of the polymer electrolyte from the resistance of both the electrodes and the electrode-membrane interfaces.<sup>13</sup>

The resistance of the electrodes ( $\sim 0.21 \Omega$ ) was estimated by measuring the short-circuited sample holder containing the two pieces of carbon cloth between the stainless steel terminal leads. The resistance of the Nafion membrane can be determined by stacking and measuring the total resistance of several identical membranes positioned between the two electrodes and subsequently removing one membrane at a time to obtain the resistance of the electrode-membranes assembly as a function of the number of membranes as shown in Fig. 2 for N105 and N115. The intercept of the curve with the y-axis corresponds to the parasitic resistances mostly associated with the electrodes and electrode-membrane interface resistances. The slope of the curve corresponds to the electrical resistance of the membrane.

The total electrical resistance of electrodes and electrode-membrane interfaces inferred from data in Fig. 2 is  $\sim 0.33 \Omega$  and  $0.37 \Omega$  for N115 and N105, respectively. The subtraction of the resistance of the electrodes ( $0.21 \Omega$ ) from

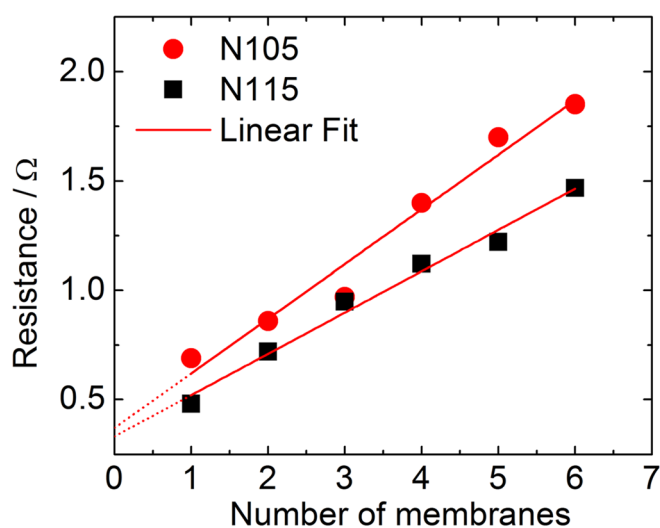


FIG. 2. Resistance of Nafion-electrodes assembly as a function of the number of stacked membranes for N105 and N115 at  $RH = 100\%$  and  $T = 25^\circ\text{C}$ .

the intercept value results in  $\sim 0.12 \Omega$  and  $\sim 0.16 \Omega$  for N115 and N105, respectively. Such values are assumed as the resistance of the electrode-membrane interface. The interface resistance is relatively large as compared to the measured electrical resistance of the membrane ( $\sim 0.20\text{--}0.30 \Omega$ ) and must be subtracted from the IS data in order to obtain accurate proton conductivity and activation energy values. Thus, the estimated proton conductivity values of N105 and N115 at  $T = 25^\circ\text{C}$  and  $RH = 100\%$  are  $\sigma \sim 0.07 \text{ S cm}^{-1}$  and  $\sigma \sim 0.10 \text{ S cm}^{-1}$ , respectively. Such values are in perfect agreement with reported Nafion conductivity data.<sup>3</sup> It is interesting to note that the reported proton conductivity measured in the in-plane configuration for N115 is  $\sigma (T = 30^\circ\text{C}) \sim 0.10 \text{ S cm}^{-1}$ ,<sup>3</sup> which is very similar to the value obtained in the through-plane configuration from Fig. 2. Such result indicates that the proton conductivity in hydrated Nafion membranes is isotropic. Considering that hydrophilic phase is ubiquitously distributed in the polymer matrix, it is reasonable to expect that the proton conduction occurs more isotropically via structural and vehicular diffusion in wet membranes, whereas effects due to the anisotropic structure of Nafion are more pronounced in the dry state.

Fig. 3 shows the Arrhenius plots of N115 for proton conductivity both in the in-plane and through-plane configurations at  $RH = 100\%$ .

The electrical conductivity measured in the home-made sample holder at constant relative humidity shows that the proton conductivity increases continuously with increasing temperature in the entire range investigated. This result is in good accordance with water uptake measurements performed with increasing  $T$  at constant  $RH = 100\%$ , which showed that the water uptake increases with increasing temperature in the  $30\text{--}140^\circ\text{C}$  range.<sup>7</sup> In contrast, the temperature dependence of the proton conductivity measured in-plane with the commercial sample holder shows a different behavior at high  $T$ , which resembles several previously reported data in which the decrease of proton conductivity of Nafion at high temperature is usually attributed to water removal.<sup>3,16,17</sup> At  $T = 180^\circ\text{C}$ , the proton conductivity in the through-plane configuration reaches  $\sigma \sim 0.4 \text{ S cm}^{-1}$ , while for the

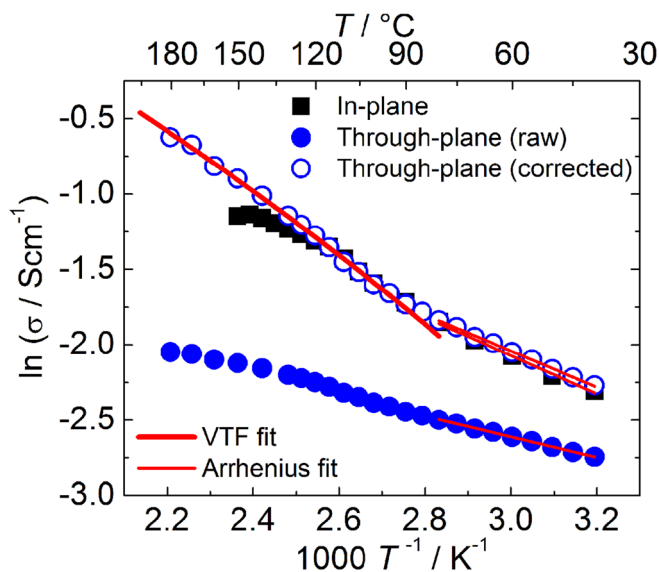


FIG. 3. Arrhenius plots of N115 proton conductivity in the in-plane, using a commercial sample holder, and in the through-plane configuration (raw data and corrected data, obtained by subtracting the resistance due to membrane-electrode interface). The continuous lines represent the Arrhenius ( $T \sim 40\text{--}90^\circ\text{C}$ ) and the VTF ( $T \sim 90\text{--}180^\circ\text{C}$ ) best fittings.

measurements in the temperature range of  $\sim 100\text{--}160^\circ\text{C}$  under constant water partial pressure, the proton conductivity drops from  $\sigma \sim 10^{-1}$  to  $10^{-3}$  S  $\text{cm}^{-1}$ .<sup>3</sup>

In the  $40\text{--}90^\circ\text{C}$   $T$  range, the proton conductivities measured in both configurations (in- and through-plane) are comparable and described by an Arrhenius-type process. The activation energies  $E_a$  of the linear portion of the curve ( $40 \leq T \leq 90^\circ\text{C}$ ) in the in-plane and through-plane raw data are  $E_a \sim 0.11$  eV and  $0.06$  eV, respectively. However, the corrected through-plane data, from which the resistance of electrode-membrane interfaces was subtracted, exhibit proton conductivity and activation energy values ( $E_a \sim 0.10$  eV) very close to the ones observed in the in-plane configuration. Such value is in good accordance with the structural diffusion of protons in aqueous media.<sup>3,13</sup> In the in-plane configuration, the resistance of the electrode-membrane interfaces is negligible as compared to the membrane resistance ( $\sim 100\text{--}1000 \Omega$ ).<sup>12</sup>

For  $T > 90^\circ\text{C}$ , a pronounced increase with a deviation from the thermally activated Arrhenius process is observed.<sup>14,15</sup> However, in- and through-plane data deviate from each other at  $T > 120^\circ\text{C}$ . With increasing temperature, in-plane curve progressively deviates from the through-plane data showing a different temperature dependence. A maximum conductivity for the in-plane data is measured at  $T = 140^\circ\text{C}$ , above which the conductivity decreases with increasing temperature. Several previously reported conductivity data exhibit similar behavior.<sup>3,16,17</sup> However, such a decrease of the conductivity is in contradiction with the observed water uptake dependence on the temperature and cannot be ascribed to other intrinsic properties of Nafion, such as morphology changes induced by the  $\alpha$ -relaxation. The data set of Fig. 3 demonstrate that the decrease of proton conductivity in Nafion usually observed at high temperature is mostly due to limitations of measuring apparatus, which cannot sustain constant RH at high temperature. The water leakage of the commercial (in-plane) sample holder was confirmed by the loss of water from the water reservoir during conductivity measurements.

The non-Arrhenius temperature dependence of the proton conductivity at  $T > 90^\circ\text{C}$  has been previously observed for Nafion membranes and has been fitted using Vogel-Tamman-Fulcher (VTF) empirical law<sup>14,15</sup>

$$\sigma = \sigma_\infty e^{\frac{-E_a}{R(T-T_0)}}, \quad (1)$$

where  $R$  is the gas constant,  $T$  is the absolute temperature, and  $T_0$  is the Vogel temperature.<sup>15</sup> The calculated activation energy for the corrected through-plane data is  $E_a = 0.09$  eV. The Vogel temperature used in the VTF fitting is  $T_0 = -138^\circ\text{C}$ . Such  $T_0$  is usually  $100$  K lower than the glass transition temperature  $T_g$  of the polymer.<sup>15</sup> The Vogel temperature used in the fitting is in good agreement with reported  $T_g \sim -20^\circ\text{C}$  of Nafion.<sup>18</sup> Although good fittings are obtained with VTF law, some important aspects have to be considered. In Nafion samples with high water content, the upturn of the proton conductivity cannot be directly ascribed to the coupling between ion conductivity and the glass transition, usually observed in amorphous (intrinsic) ion conductors.<sup>17</sup> In addition, it was previously reported that the water uptake of autoclaved Nafion membranes immersed in water increases at  $T > 100^\circ\text{C}$ .<sup>7</sup> As the proton conductivity is strongly sensitive to the membrane water content,<sup>22</sup> the increased proton conductivity at high  $T$  can be related to a pronounced swelling, which can be associated with either an increase of the polymer free volume at  $T > T_g$  or a structural destabilization of the polymer matrix at  $T$  above the  $\alpha$ -relaxation.<sup>7,15</sup> Recent studies revealed that Nafion samples undergo morphological changes (shape memory) that are controlled by the  $\alpha$ -relaxation ( $T_\alpha \sim 110^\circ\text{C}$ ).<sup>19-21</sup> The change of the water content upon heating and the thermal transitions of Nafion cast doubts on the VTF law and indicate that further studies are necessary to better clarify the origin of the proton conductivity upturn at high  $T$ .

In order to evaluate the influence of structural changes on Nafion proton conductivity, Fig. 4 shows the Arrhenius plots for N105 in two successive heatings. In the first

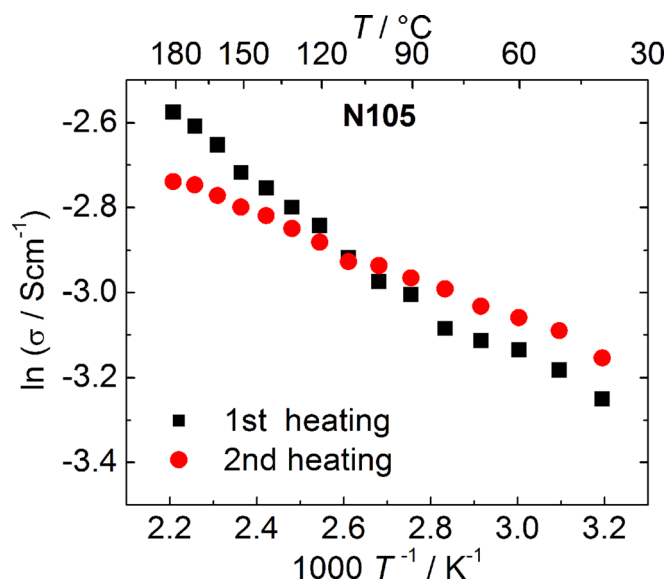


FIG. 4. Arrhenius plots of N105 proton conductivity (raw data) in the through-plane configuration collected in two successive heatings.

heating, proton conductivity of N105 shows similar temperature dependence as N115 (Fig. 3), with two regimes separated at  $T \sim 90^\circ\text{C}$ . Nonetheless, conductivity curve collected during the second heating reveals a different behavior. The deviation from the Arrhenius-like dependence for  $T > 90^\circ\text{C}$  is not observed and the data follow a more linear dependence over the entire  $T$  range investigated. The different temperature dependence of the proton conductivity observed between the first and second heating can be a result of structural changes occurring in the ionomer matrix during the first heating. This behavior is in accordance with the reported structural transition taking place in Nafion membranes for  $T > T_\alpha$ ,<sup>20,21</sup> and further suggests that the VTF law is not suitable for describing the thermal dependence of proton conductivity at high  $T$ .

In summary, the proton conductivity of Nafion membranes was evaluated in a wide temperature range at high relative humidity. The proton conductivity increases in the entire temperature range, in agreement with the water uptake measured at high temperature. Two distinct thermally activated processes were observed for the proton conductivity in the first heating: Arrhenius temperature dependence for  $T < 90^\circ\text{C}$ , and for  $T > 90^\circ\text{C}$  an upturn of the proton conductivity deviates the temperature dependence from the Arrhenius behavior. However, structural changes due to thermal history prevented the reversibility of the proton conduction. The proton conductivities in the in- and through-plane configurations were found to be very similar indicating isotropic conductivity in fully hydrated Nafion membranes.

Thanks are due to the Brazilian funding agencies (CAPES, CNPQ, FAPESP) and CNEN.

- <sup>1</sup>K. A. Mauritz and R. B. Moore, *Chem. Rev.* **104**, 4535–4585 (2004).
- <sup>2</sup>D. Kim, K. J. Kim, Y. Tak, D. Pugal, and H.-S. Park, *Appl. Phys. Lett.* **90**, 184104 (2007).
- <sup>3</sup>K. D. Kreuer, M. Schuster, B. Obliers, O. Diat, U. Traub, A. Fuchs, U. Klock, S. J. Paddison, and J. Maier, *J. Power Sources* **178**, 499–509 (2008).
- <sup>4</sup>K. D. Kreuer, M. Ise, A. Fuchs, and J. Maier, *J. Phys. IV (France)* **10**, Pr7-279–Pr7-281 (2000).
- <sup>5</sup>K. Schmidt-Rohr and Q. Chen, *Nature Mater.* **7**, 75 (2008).
- <sup>6</sup>M. Marechal, J.-L. Souquet, J. Guindet, and J.-Y. Sanchez, *Electrochem. Commun.* **9**, 1023–1028 (2007).
- <sup>7</sup>K. D. Kreuer, *Solid State Ionics* **252**, 93–101 (2013).
- <sup>8</sup>B. R. Matos, R. A. Isidoro, E. I. Santiago, M. Linardi, A. S. Ferlauto, A. C. Tavares, and F. C. Fonseca, *J. Phys. Chem. C* **117**, 16863–16870 (2013).
- <sup>9</sup>J. R. Bunn, D. Penumadu, R. Woracek, N. Kardjilov, A. Hilger, I. Manke, and S. Williams, *Appl. Phys. Lett.* **102**, 234102 (2013).
- <sup>10</sup>B. R. Matos, M. A. Dresch, E. I. Santiago, M. Linardi, D. Z. de Florio, and F. C. Fonseca, *J. Electrochem. Soc.* **160**, F43–F48 (2013).
- <sup>11</sup>G. Alberti, M. Casciola, L. Massinelli, and B. Bauer, *J. Membr. Sci.* **185**, 73 (2001).
- <sup>12</sup>C. H. Lee, H. B. Park, Y. M. Lee, and R. D. Lee, *Ind. Eng. Chem. Res.* **44**, 7617–7626 (2005).
- <sup>13</sup>J. Halim, F. N. Büchi, O. Hass, M. Stamm, and G. G. Scherer, *Electrochim. Acta* **39**, 1303–1307 (1994).
- <sup>14</sup>G. Xu and Y. S. Pak, *J. Electrochem. Soc.* **139**, 2871 (1992).
- <sup>15</sup>J. J. Fontanella, M. G. Mclin, and M. C. Wintersgill, *J. Polym. Sci., Part B: Polym. Phys.* **32**, 501 (1994).
- <sup>16</sup>M. Casciola, G. Alberti, M. Sganappa, and R. Narducci, *J. Power Sources* **162**, 141–145 (2006).
- <sup>17</sup>V. Di Noto, R. Gliubbizzi, E. Negro, and G. Pace, *J. Phys. Chem. B* **110**, 24972–24986 (2006).
- <sup>18</sup>S. J. Osborn, M. K. Hassan, G. M. Divoux, D. W. Rhoades, K. A. Mauritz, and R. B. Moore, *Macromolecules* **40**, 3886 (2007).
- <sup>19</sup>B. R. Matos, E. I. Santiago, J. F. Q. Rey, A. S. Ferlauto, E. Traversa, M. Linardi, and F. C. Fonseca, *J. Power Sources* **196**, 1061–1068 (2011).
- <sup>20</sup>K. A. Page, J. K. Park, R. B. Moore, and V. G. Sakai, *Macromolecules* **42**, 2729–2736 (2009).
- <sup>21</sup>T. Xie, K. A. Page, and S. A. Eastman, *Adv. Funct. Mater.* **21**, 2057–2066 (2011).
- <sup>22</sup>K. D. Kreuer and G. Portale, *Adv. Funct. Mater.* **23**, 5390–5397 (2013).